

Novel method for in-situ drift velocity measurement in large volume TPCs: the Geometry Reference Chamber of the NA61/SHINE experiment at CERN

András László,^{a,*} Ádám Gera,^{a,b} Gergő Hamar,^a Botond Pálfi,^{a,c} Piotr Podlaski,^d Brant Rumberger,^{e,f} and Dezső Varga^a

^a*HUN-REN Wigner Research Centre for Physics, Budapest, Hungary*

^b*Current affiliation: GSI, Darmstadt, Germany*

^c*Eötvös University, Budapest, Hungary*

^d*University of Warsaw, Warsaw, Poland*

^e*University of Colorado Boulder, Boulder, CO, USA*

^f*Current affiliation: Trimble Inc., Westminster, CO, USA*

**Corresponding author.*

E-mail: laszlo.andras@wigner.hun-ren.hu, gera.adam@wigner.hun-ren.hu,
hamar.gergo@wigner.hun-ren.hu, palfi.botond@gmail.com,
piotr.podlaski@cern.ch, brant.rumberger@gmail.com,
varga.dezso@wigner.hun-ren.hu

ABSTRACT: This paper presents a novel method for low maintenance, low ambiguity in-situ drift velocity monitoring in large volume Time Projection Chambers (TPCs). The method was developed and deployed for the 40 m³ TPC tracker system of the NA61/SHINE experiment at CERN, which has a one meter of drift length. The method relies on a low-cost multi-wire proportional chamber placed next to the TPC to be monitored, downstream with respect to the particle flux. Reconstructed tracks in the TPC are matched to hits in the monitoring chamber, called the Geometry Reference Chamber (GRC). Relative differences in positions of hits in the GRC are used to estimate the drift velocity, removing the need for an accurate alignment of the TPC to the GRC. An important design requirement on the GRC was minimal added complexity to the existing system, in particular, compatibility with Front-End Electronics cards already used to read out the TPCs. Moreover, the GRC system was designed to operate both in large and small particle fluxes. The system is capable of monitoring the evolution of the drift velocity inside the TPC down to a one permil precision, with a few minutes of data collection.

KEYWORDS: Time projection chambers (TPC), Particle tracking detectors (Gaseous detectors), Large detector systems for particle and astroparticle physics

ARXIV EPRINT: [2405.01285](https://arxiv.org/abs/2405.01285)

Contents

1	Introduction	1
2	The NA61/SHINE experimental facility	3
3	The GRC system	5
4	Drift velocity calibration using the GRC	7
5	Concluding remarks	11
A	Trigger delay and drift-direction alignment of TPCs	13
B	Systematic errors and alignment calibration of the TPCs	14

1 Introduction

The NA61 experiment, also called the SPS Heavy Ion and Neutrino Experiment (SHINE) [1], is a large-acceptance hadron spectrometer experiment at the Super Proton Synchrotron (SPS) accelerator at CERN. Its physics program includes measurements for heavy-ion physics, as well as measurements on particle production in hadron-nucleus collisions, with an emphasis on the application of those measurements in flux predictions for long-baseline neutrino oscillation experiments (T2K, DUNE, NOvA, Hyper-Kamiokande) [2–5] and for cosmic ray observatories (such as Pierre Auger Observatory) [6]. These physics programs demand the operation of NA61/SHINE in both high and low particle multiplicity environments.

The main components of the NA61/SHINE experiment are two large superconducting bending magnets and a system of large volume Time Projection Chambers (TPCs). As the drift dimension of the TPCs is considerably large ($\gtrsim 1$ meter), in order to achieve necessary position resolution in the drift direction, the drift velocity inside the TPCs needs to be monitored at the permil level. Since the drift velocity slowly evolves with time, mostly due to variations in the ambient conditions or gas composition, its evolution needs to be followed every few minutes of data taking. In this paper, we describe a cost-efficient supplementary detector system specifically developed for this purpose.

One of the default methods for monitoring drift velocity in a TPC is to analyze its exhaust gas with a small probe chamber [1, 7–9] and then predict the drift velocity inside the TPC via the known pressure, temperature and drift field in the TPC gas. This method dates back to the large-volume TPCs of ALEPH and DELPHI at LEP [10, 11]. NA61/SHINE also uses this technique to monitor the drift velocity in its TPCs, but due to the limited absolute systematic accuracy of the method, it is mainly used for monitoring the time stability of the gas composition.¹ The exhaust method

¹The so-called normalized drift velocity, estimated via exhaust analyzer, is the hypothetical drift velocity extrapolated to a fixed pressure, fixed temperature, and to a fixed drift field. That quantity, although is not directly related to the actual drift velocity inside the TPC, but is rather useful for monitoring the time stability of the working gas composition.

is prone to uncertainties in pressure and temperature measurements in the large-volume chambers, and is also vulnerable to contaminations along the exhaust collection and system outgassing.

An other typical method applied in a number of experiments is the so-called bottom point method: the drift time of the last points of tagged cathode-exiting tracks can be used for drift velocity estimation, provided that the delay of the trigger signal to the TPC readout is known to a good accuracy, along with a precise estimate for the effective drift length. In NA61/SHINE we do not rely on this method, primarily because it is prone to systematic uncertainties of the effective drift length, but more importantly of the trigger delay, which is not even known a priori. A further method, often applied in large volume TPC experiments, relies on imaging start and end points of cosmic ray tracks. In NA61/SHINE, such method is not suitable, as the orientation of the TPC acceptance and drift direction is suboptimal with respect to the celestial directions, leading to large uncertainties in the cosmic track start and end point reconstruction.

Due to the systematic uncertainties of the above approaches, a more advanced absolute in-situ drift velocity measurement method is needed. For such purpose, typically a UV laser system is used: ionizing laser beam tracks are projected into the sensitive volume at known locations, and the drift velocity can then be measured from the apparent positions of these beams in terms of TPC drift time. Direct measurement methods using laser systems are common [8, 12] and very accurate. UV laser-based drift velocity and geometry monitoring systems, however, are rather hard to implement or upgrade on existing chambers retrospectively. Moreover, the cost and development time for such systems is substantial. NA61/SHINE is not equipped with such a UV laser based system.

Along with other CERN experiments, the NA61/SHINE facility was also significantly upgraded during the Long Shutdown 2 (LS2) period (2019-2021) of the accelerator complex. Since during the LS2 the subdetectors were moved, precise alignment calibration of the chambers was required, as was a system for accurately and reliably determining their drift velocities. As the TPCs were already constructed, minimally-invasive measurement systems were preferred. Our choice was a simple solution: a planar detector with fixed segmentation along the TPC drift direction, called the Geometry Reference Chamber (GRC), was to be placed downstream of the TPC system with respect to the particle flux. TPC tracks reconstructed with an approximately known drift velocity are extrapolated to the GRC and paired with the GRC hits. If the drift velocity estimate differs from the true drift velocity inside the TPC, the mismatch of the drift coordinate of the hits becomes worse with increasing drift depth. The ratio between the initial approximate drift velocity and the actual drift velocity in the chamber can then be estimated from the slope of this mismatch scatter plot. That is, the GRC is used as a differential length scale in order to convert the drift time, measured by the TPC readout, to drift depth. It is quite advantageous that the GRC method is differential: an accurate alignment of the TPC against the GRC is not needed. The concept is illustrated in Fig.1.²

In order to implement the GRC concept, several design requirements were considered. To reduce the development time and cost of the readout electronics, a solution using the existing TPC readout Front-End Electronics (FEE) was chosen. To reduce the number of readout channels, we decided to implement a simple planar Multi-Wire Proportional Chamber (MWPC) with Cartesian

²Once the drift velocity has been calibrated with such method in one of the TPC chambers in the detector complex, the other chambers can be calibrated against each-other, using the already calibrated chambers as geometry reference. Moreover, the remaining geometry calibration constants of the TPC system can also be estimated, such as the trigger delay (t_0), alignment shift and alignment angles for each chamber, see Appendix A and B.

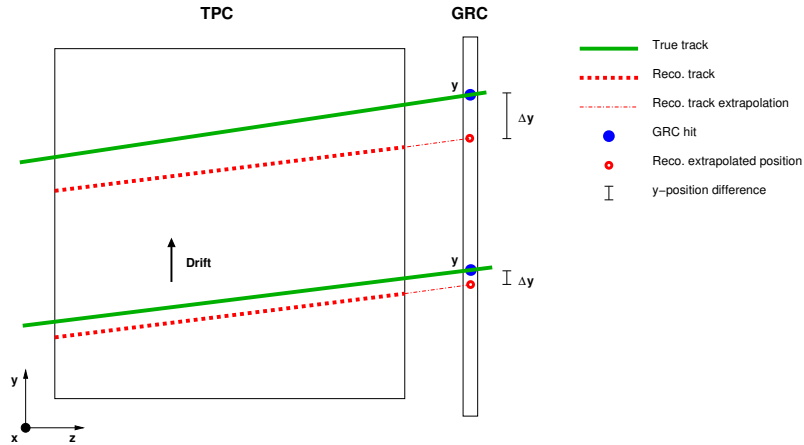


Figure 1. (Color online) Illustration of the Geometry Reference Chamber (GRC) concept. The particle tracks in the TPC chamber are reconstructed with an initial estimate for the drift velocity and are paired to the hits of a segmented detector, the GRC. In case the initial approximate drift velocity estimate differs from the true drift velocity inside the TPC, the mismatch along the drift coordinate gets gradually worse at increasing drift depths. The slope of the drift coordinate mismatch against the drift coordinate as measured by the GRC provides the estimate for the corresponding multiplicative correction factor. (The figure shows the projection orthogonal to the magnetic bending plane, in case the TPC is used in a magnetic spectrometer experiment, such as the NA61/SHINE.)

readout. This setting required two issues to be addressed. Firstly, the signal formation in the GRC had to be slowed down sufficiently such that the signal persists until the TPC electronics begins to sample the charges. This is not entirely trivial to achieve, since TPC readout electronics typically allow for a microsecond-level trigger delay with respect to the particle passage time, during which the signal may already disappear from the GRC. In order to mitigate this issue, a drift volume with adjustable drift field was introduced in the GRC design, transverse to the particle passage direction, and with that the GRC signal duration could be controlled. Secondly, the Cartesian readout scheme tends to be problematic whenever the particle occupancy is large. In order to overcome this limitation, the GRC acceptance was designed to be variable: for low-multiplicity collisions, the entire GRC acceptance can be used, whereas for high-multiplicity collisions, individual anode wires (sense wires) of the GRCs can be disabled, down to a single amplifying wire. This helps to reduce the number of combinatorial ghost hits.

The structure of the paper is as follows. In Section 2 an overview of the NA61/SHINE experimental facility is given. In Section 3 the GRC design requirements, parameters, and implementation are discussed. In Section 4 the operational performance is shown. In Section 5 a conclusion is provided. Appendices A and B discuss some details of systematic errors and the estimation of further geometry-related TPC calibration constants, where the GRC chamber plays a role.

2 The NA61/SHINE experimental facility

The NA61/SHINE [1] is a fixed-target hadron spectrometer experiment at the CERN SPS accelerator. Large parts of its tracking devices were inherited from a previous experiment called NA49 [8].

Its physics program covers the study of strongly-interacting matter via heavy-ion collisions, and measurements of identified particle production spectra in hadron-nucleus collisions as reference data for flux prediction in long baseline neutrino experiments and large area cosmic ray observatories.

An overview of the NA61/SHINE experiment is shown in Fig.2. Two large superconducting bending magnets (Vertex-I and II) are responsible for particle deflection for charge and momentum determination. Their total maximum bending power is $\sim 9 \text{ Tm}$ (up to 1.5 Tesla magnetic field in Vertex-I and 1.1 Tesla in Vertex-II). A target holder with target-in / target-out moving capability sits just upstream of the first Vertex TPC, upstream/downstream always meant with respect to the beam direction throughout the paper. Thin targets can be placed inside a silicon Vertex Detector (VD) for precise vertex determination. NA61/SHINE also has the ability to measure interactions in extended replica targets for long baseline neutrino experiments. The tracking devices for spectrometry are composed of eight large volume TPCs (total $\sim 40 \text{ m}^3$ and $\sim 1 \text{ m}$ drift length), capable of performing both tracking and dE/dx measurements. A Multigap Resistive Plate Chamber (MRPC) based Time-of-Flight wall (L-ToF) provides further particle identification (PID) capabilities around mid-rapidity, whereas a scintillator based Time-of-Flight wall (F-ToF) covers the forward phase space, enabling two-dimensional (ToF+ dE/dx) separation of particle species at large parts of the acceptance. A calorimeter is placed at the end of the beamline, called the Projectile Spectator Detector (PSD), which helps to characterize collision centrality in heavy-ion collisions, and consists of two compartments (Main- and Forward-PSD, also called MPSD and FPSD) for optimal shower containment. Upstream of the target position, a set of beam position detectors (BPDs) provide beam tracking information, while scintillator and Cherenkov detectors serve as beam trigger with PID capability (not shown in the figure). On the beamline between VTPC-1 and the GapTPC, a small plastic scintillator with a 1 cm diameter serves as an interaction trigger in most collision types (S4). In rare run settings, a very similar scintillator (S5) just upstream of MPSD is used instead. For heavy-ion runs, the scintillator (S3) just downstream of VD is used for interaction definition through detecting loss of charge (i.e., by sensing a decreased Z^2 with respect to the beam nuclei). The VD, the new silicon BPDs, the MRPC-based L-ToF, the MPSD and FPSD were introduced during the LS2 upgrade period between 2019-2021. Also during LS2, the data acquisition (DAQ) was upgraded, allowing for an event recording rate up to 1.8 kHz for the detector complex.

The concept of the Geometry Reference Chambers (GRCs), just downstream of MTPC-L, was also developed during the LS2 upgrade period. Its lightweight design was motivated by short development time, and relatively fast and low risk implementability. In addition, the TPCs were moved during the LS2 upgrade, and therefore seven calibration constants apart from the drift velocity must be re-determined for each TPC. These are the trigger delay, the three-dimensional alignment shifts, and the three alignment angles, per chamber, independently. The large number of unknown calibration constants are hard to determine without an absolute reference. The GRC enables unambiguous determination of all seven parameters and the drift velocity, for each component of the TPC system.

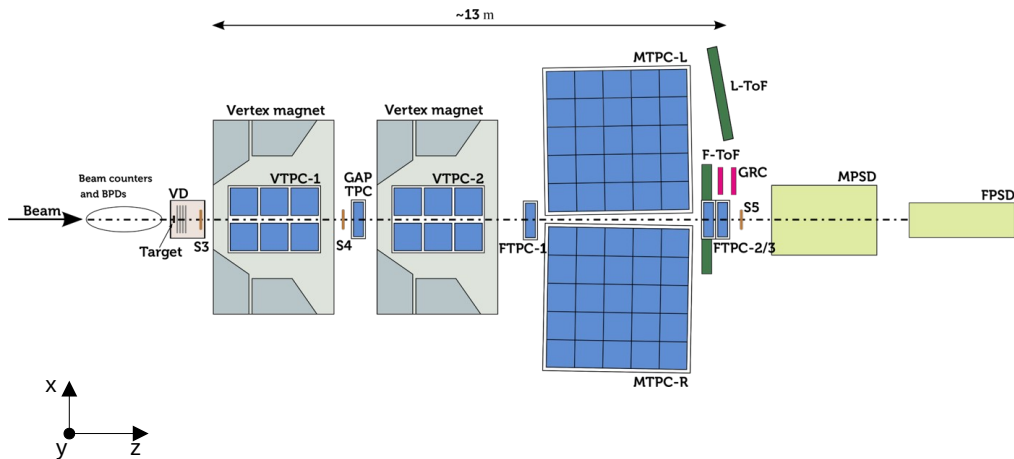


Figure 2. (Color online) The NA61/SHINE detector configuration, after the Long Shutdown 2 (LS2) upgrade, i.e. since 2022. The drawing shows the top view of the bending plane. That is, the approximately homogeneous magnetic field inside the Vertex-I and Vertex-II magnets is perpendicular to the figure ($\sim y$ axis). The electric drift field of the TPCs is also perpendicular to the figure ($\sim y$ axis). The GRC system for in-situ drift velocity monitoring was also conceptualized and introduced during the LS2. The GRC system, as of now, consists of two adjacent identical chambers (GRC-1 and GRC-2), for redundancy reasons. As the figure is a top view of the experiment, the shorter dimension of the GRCs is seen in this outline.

3 The GRC system

The NA61/SHINE TPCs have a drift length of ~ 1 m and are capable of resolving particle cluster positions at the ~ 1 mm at the extremum of the drift volume. Therefore, in order to reduce the systematic errors of the position measurements below the position resolution, the drift velocity has to be determined with permil accuracy. The drift velocity in a typical TPC system is affected by the working gas composition, the electric drift field applied to the TPC, the gas temperature, and the gas pressure. Most large TPC systems, such as the TPCs in NA61/SHINE experiment or the one in ALICE [12] at CERN's LHC, or in STAR [13, 14] at BNL's RHIC, are equilibrated with the atmospheric pressure, with a very slight constant overpressure applied in order to avoid air infiltration. Since the gas composition, drift field and the temperature is typically stabilized, the shortest time scale variations are caused by meteorological changes in the ambient air pressure. This means that the time scale of anticipated substantial drift velocity variations are not shorter than about 5 minutes. Therefore, the design goal of the GRC system was to have a drift velocity measurement inside MTPC-L with a permil statistical error for about every 5 minute time window during data taking. Given the worst-case minimal particle flux, this requirement gives the lower bound to the acceptance (area) of the GRC in case of low-multiplicity collision types. In order to minimize the necessary area of the GRC, a location was chosen with the maximum possible particle flux passing through MTPC-L, but avoiding the vicinity of the beam spot. This justifies the chosen placement of the GRC system, shown in Fig.2. At the selected location, the worst-case minimum particle flux was estimated using formerly recorded proton-proton collision data at 13 GeV/c beam

momentum. With about a factor of two safety margin, this resulted in a $40\text{ cm} \times 120\text{ cm}$ sensitive area, with the longer dimension fully covering the drift direction of MTPC-L. For redundancy reasons, two identical GRC stations (GRC-1 and GRC-2) were placed in an adjacent position (see Fig.2).

For cost efficiency reasons, the GRC implementation was chosen to be a robust MWPC with Cartesian readout loosely based on the design [15, 16], which was originally optimized for cosmic muon imaging purposes. Gas amplification is achieved on the anode wires (sense wires), and the transverse position information is read from adjacent wires (field wires) parallel to these in the same plane. For the vertical position information relevant for drift velocity monitoring, the segmentation is achieved using wires with the same functionality as cathode strips, perpendicular to the sense wire / field wire direction (those are called pickup wires). The design choice to use such wires instead of strips is due to easier construction of the whole chamber. For low-multiplicity data taking campaigns, the entire GRC acceptance is read out as is. For high-multiplicity runs, such as heavy-ion data taking periods, the Cartesian combinatorial background becomes an issue. In order to mitigate this, the design allows for high-voltage jumpers used to turn off individual sense wires: the sense wires can be connected either to their operational voltage or to the chamber ground. The jumpers are configured manually at the start of a data taking campaign. Turning off sense wires has the effect of narrowing the transverse acceptance, eventually down to a single active sense wire. This feature completely eliminates the Cartesian combinatorics, preserving the drift velocity determination accuracy in high multiplicity runs. The concept is sketched in the left panel of Fig.3.

In order to reduce cost and development time for the readout electronics, the GRCs were designed to be read out using the existing TPC FEEs. Two TPC FEE cards are enough to read out the induced charges on the $32\text{ field wire channels} \times 192\text{ pickup wire channels}$ in each GRC. A natural issue with this solution is that the TPC, being a relatively slow device, allows for a relatively large trigger delay. Typical TPC trigger and readout electronics are only optimized for making meaningful charge sampling measurements $1 - 2\ \mu\text{s}$ after the beam passage. This relatively large but constant time delay is due to trigger logic decision time, signal arrival time on the signal cables, as well as the startup time of the FEE logic. In order to make sure that the signal in the GRC persists until the TPC FEE begins to take meaningful charge samples, a 30 mm thick drift volume was added. This has the effect of extending charge collection over time. In order to control the signal collection timescale, an adjustable drift field electrode was added to the design. The signal stretching concept is shown schematically in the right panel of Fig.3.³ The GRC front-end readout system is fully integrated with the NA61/SHINE Data Acquisition System (DAQ). GRC-specific event reconstruction software is fully integrated with the NA61/SHINE offline software (ShineOffline) [17]. The fundamental parameters of the MWPC design of the GRCs are listed in Table 1.

Since the GRC performs a differential measurement along the TPC drift direction, precise

³Due to the mentioned thickened charge collection volume, the charge collection direction slightly differs from the the particle incidence direction in case of tracks arriving non-orthogonally at the GRC surface. This causes a small angle-dependent position bias, which can be easily corrected for, using the incidence angles estimated by the TPC track piece. Due to the NA61/SHINE geometry, the pertinent bias is of the order of $\sim 1\text{ mm}$ at the extremes, and vanishes toward the middle of the GRC acceptance. Moreover, in the NA61/SHINE geometry, this bias is second order, therefore it happens to cancel in the GRC-based drift velocity calibration procedure.

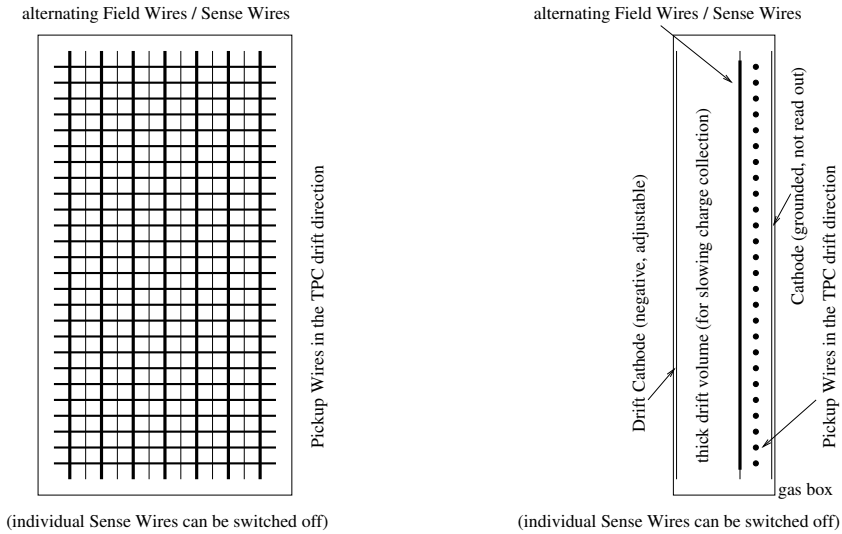


Figure 3. Left panel: sketch of a GRC chamber as seen from the direction of the arriving particle flux (not to scale). The transverse direction is covered by the field wire / sense wire plane, where the electron multiplication takes place on the sense wires, and their mirror charges on the field wires are read out. The TPC drift direction is covered by the pickup wire plane, also seeing the mirror charges of the charge clouds on the sense wires. This provides the other Cartesian coordinate for readout. Individual sense wires can be connected to high voltage or ground using configurable high-voltage jumpers (not drawn on the figure). Right panel: sketch of a GRC as seen from side view (not to scale). The thickness of the drift region is larger in the direction of the particle flux, and a drift cathode electrode with adjustable potential is used. This combination makes sure that the charge collection can be sufficiently slowed down such that the signal in the chamber persists until the TPC readout electronics, used for the GRC readout, begins to measure.

alignment of the GRCs with respect to the TPC is not critical. However, if the TPC-GRC alignment is known, the GRC system can be used to determine a further calibration constant: the trigger delay (t_0). In order to make use of this possibility, care was taken in the design that the position of the optical survey target for geodesic localization of the GRCs can be accurately related to the internal wire positions. A CAD sketch of the sensor plane and a photograph of the installed GRC system is seen in Fig.4.

4 Drift velocity calibration using the GRC

Drift velocity calibration via the GRC is based on track matching between MTPC-L and the GRC as sketched in Fig.1, and subsequently using GRC as a differential length scale.⁴ If the drift velocity estimate differs from the true drift velocity, the TPC drift coordinate versus GRC coordinate mismatch has a slope as a function of the GRC coordinate. This slope can be used for calibration.

⁴For combinatorial background suppressing reasons, in practice global tracks are used, which are associated to a collision in the target (global main-vertex tracks). These can be already reconstructed with approximate estimates for the calibration parameters, such as the drift velocity. Then, these global main-vertex tracks are dissected to local tracks, and the parameter mismatch of the local track pieces in the adjacent TPC chambers are evaluated for calibration. For MTPC-L, the mismatch against the GRC hits are used for calibration.

chassis	FR4 bars and typical PCB board material
typical working gas	Ar(80) : CO ₂ (20) at 5 l/h flow
typical drift cathode potential	0 V
field wire and pickup wire potential	0 V
typical sense wire potential	1580 V
pickup wire	CuZn40 (EDM Tec) 100 μ m, 70 g tension
field wire	CuZn40 (EDM Tec) 100 μ m, 70 g tension
sense wire	Au coated W (Luma Metall) 20 μ m, 15 g tens.
field wire to sense wire distance	6 mm
distance between adjacent pickup wires	3 mm (read out pairwise)
FW/SW to pickup wire plane distance	10 mm
pickup wire plane to cathode backplane dist.	2 mm
drift cathode to FW/SW plane	30 mm
number of sense wires	31
number of field wires	32
number of pickup wire pairs	192

Table 1. Design parameters of the GRC MWPCs.

Tracks are typically collected over the course of 5 minutes of data taking, providing a drift velocity estimate spanning those 5 minutes.

The calibration equations can be derived as follows. The NA61/SHINE coordinate convention, as seen in Fig.2, is that the global Cartesian x coordinate is from MTPC-R to MTPC-L, the global y coordinate is from down to up, and the global z coordinate is along the nominal beamline from upstream toward downstream. Similarly oriented x , y , z Cartesian local coordinates are also used within each chamber. The TPC drift coordinate is the y local coordinate, by convention, and the drift is from negative to positive direction, whereas the local x coordinate is along the readout pads of a pad row (along the sense wires of the TPC), and the local z coordinate is stepping in between pad rows. For a TPC chamber, one has that

$$\begin{aligned}
y_{\text{nom}} &= y_{\text{anode,nom}} - (t_{0,\text{nom}} + t_{\text{drift,raw}}) \cdot v_{\text{drift,nom}}, \\
y_{\text{true}} &= y_{\text{anode,true}} - (t_{0,\text{true}} + t_{\text{drift,raw}}) \cdot v_{\text{drift,true}}.
\end{aligned}
\tag{4.1}$$

Here y_{nom} is the reconstructed drift coordinate assuming a nominal estimate during reconstruction for the position of the TPC amplification plane at $y_{\text{anode,nom}}$, the anode meaning the field wire / sense wire plane of the TPC. The symbol $t_{0,\text{nom}}$ stands for a nominal estimate for the trigger delay during reconstruction. $t_{\text{drift,raw}}$ is the measured particle track cluster position in terms of drift time as measured by the TPC readout. $v_{\text{drift,nom}}$ is the nominal estimate for the electron drift velocity in the TPC during reconstruction. The quantities labeled by $()_{\text{true}}$ are the true but unknown values of these calibration factors. The negative sign in Eq.(4.1) is due to the coordinate convention in NA61/SHINE. The coordinate y_{nom} measured by the TPC along the drift direction corresponds to a GRC measurement y_{true} , for each track matched to a GRC hit, as seen in Fig.1. The matching is done via a typically ~ 3 cm wide tolerance window. By eliminating the running variable $t_{\text{drift,raw}}$ in

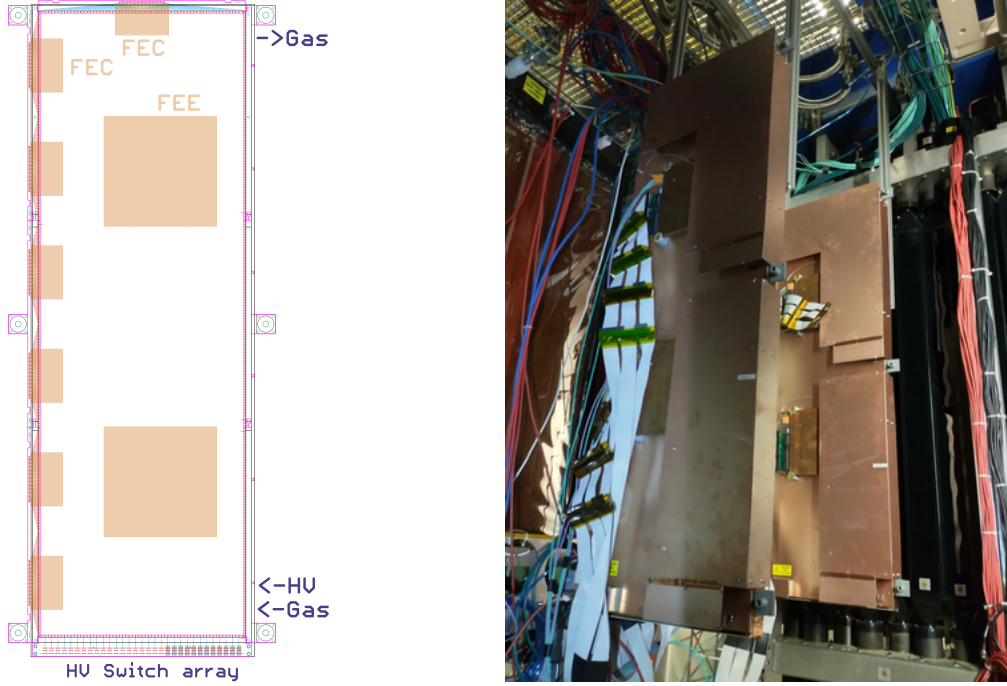


Figure 4. (Color online) Left panel: the PCB CAD snapshot of the sensor layer of a GRC chamber. The six holders for the optical geodesic survey targets are well visible. By design, these are precisely related to the internal wire geometry. Right panel: the photograph of the installed GRC system as seen looking upstream. The black wall is the F-TOF, covering the downstream plane of MTPC-L. The upstream chamber is GRC-1, whereas the downstream chamber is GRC-2.

Eq.(4.1), one infers

$$\Delta y = \underbrace{\left(v_{\text{drift,nom}} / v_{\text{drift,true}} - 1 \right)}_{\text{slope}} \cdot y_{\text{true}} + \underbrace{\left(y_{\text{anode,nom}} - v_{\text{drift,nom}} / v_{\text{drift,true}} \cdot y_{\text{anode,true}} + v_{\text{drift,nom}} \cdot (t_{0,\text{true}} - t_{0,\text{nom}}) \right)}_{\text{offset}} \quad (4.2)$$

for the ensemble of TPC-GRC tracks. Here $\Delta y := y_{\text{nom}} - y_{\text{true}}$ stands for the drift coordinate TPC-GRC mismatch and y_{true} stands for the GRC measurement. Occasionally, the label $(\)_{\text{true}}$ will be suppressed where not confusing. The slope of the Δy versus y scatter plot determines the correction factor between the true drift velocity $v_{\text{drift,true}}$ and the estimate $v_{\text{drift,nom}}$ assumed during the reconstruction, thus $v_{\text{drift,true}}$ can be estimated from the TPC-GRC mismatch data. This is shown in Fig.5 top panel for a typical low-multiplicity data set (proton-carbon collisions at 120 GeV/ c beam momentum, recorded in 2023). In Fig.5 bottom left panel the same is shown, but for a typical high-multiplicity data set (Pb+Pb collisions at 150 AGeV/ c beam momentum, recorded in 2022). Fig.5 bottom right panel shows the same high-multiplicity data set with only a single sense wire switched on, thus eliminating the Cartesian combinatorial ghost hits using the design feature explained in Section 3.

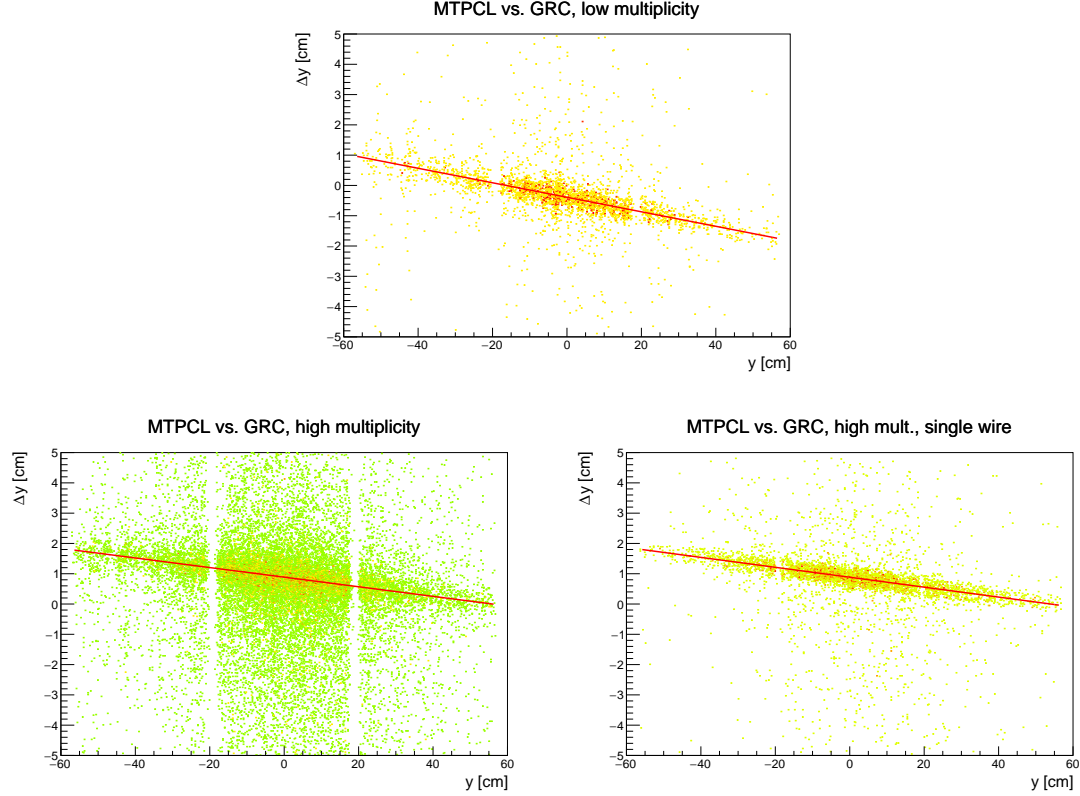


Figure 5. (Color online) Top panel: an example for the Δy versus y drift velocity calibration method on a real data sample in a 5-minute time window. The corresponding data set is a low multiplicity run (proton-carbon collisions at 120 GeV/ c beam momentum, recorded in 2023). Here, the full GRC acceptance was used. Bottom left panel: the equivalent plot for a high multiplicity run, with the full GRC acceptance (Pb+Pb collisions at 150 AGeV/ c beam momentum, recorded in 2022). Bottom right panel: the same high multiplicity data set with only a single sense wire used, thus eliminating the Cartesian combinatorial ghost hits in GRC. Note the substantially reduced background. The color scale of the scatter plot is merely to emphasize hit density for the eye. The line on the plots corresponds to a straight line fit to the scatter data, using the background tolerant LTS method. The slopes of the fitted lines yield the drift velocity correction.

In order to further suppress the combinatorial background accompanying the correlation signal, the ROOT [18, 19] implementation of the Least Trimmed Squares (LTS) fitting was used. After calibrating MTPC-L, the other chambers in the TPC system are subsequently calibrated step-by-step against each other, using the already calibrated ones as geometric reference.

The statistical uncertainty of the method can be estimated from above by treating the pickup wire electrodes as 6 mm wide strips. Thus, the single-track position resolution of the GRC is not worse than $6 \text{ mm}/\sqrt{12}$, corresponding to the resolution of a 6 mm wide uniform distribution. For a track sample of a ~ 5 minute time window, typically there are hundreds of MTPC-L tracks hitting the GRC, giving a resolution of $6 \text{ mm}/\sqrt{12}/\sqrt{N_{\text{tracks}}}$ for such ensemble of tracks. It is thus possible to push the statistical uncertainty below the desired 1 mm, corresponding to 1 per mil of the ~ 1 m TPC drift length. The systematic accuracy of the method was quantified using a closure test. By re-reconstructing the data using the calibrated drift velocities, the calculated correction on top of

the previously-corrected drift velocities was found to be better than 1-2 permil. The systematics were also double-checked by comparing the obtained drift velocities to the exhaust analysis method, which agreed within 1-2 permil, up to a scale adjustment constant. Note that the exhaust analysis method is expected to have worse systematic uncertainties, hence the need for the scale adjustment constant for the exhaust method. These validation plots are seen in Fig.6.

After calibrating the MTPC-L using the GRC, the other chambers are calibrated pairwise against each-other. Namely, the calibration scheme is MTPC-L from GRC, followed by VTPC-2 from MTPC-L, then MTPC-R from VTPC-2, and VTPC-1 from VTPC-2, and so on. Once having a methodology for drift velocity calibration, it is possible to extract further calibration constants from the data. Namely, it is possible to estimate the the trigger delay (t_0) and the drift direction displacement (y_0) of a chamber, see Appendix A. Moreover, using magnetic field-off calibration data, it is possible to estimate the chamber alignment parameters, as explained in Appendix B. A detailed systematic error analysis is also provided there. It is worth to note that after the above drift velocity and geometry calibration procedure, the magnetic field-off data are also used to map out the electric drift field distortions inside the TPCs: residuals of refitted local tracks are tabulated as a function of space, and are used as a fine-correction. At the boundaries, these residuals are up to ~ 1 mm and are much smaller inside the volumes. The drift field distortion corrections are of second order, and therefore do not interfere with the discussed drift velocity and geometry calibration.

5 Concluding remarks

In this paper a novel cost-efficient method was described for in-situ drift velocity monitoring in large volume TPCs. The method was deployed and is currently in use at the NA61/SHINE experiment at CERN. The key idea is to place a low-cost segmented detector, called to be the Geometry Reference Chamber (GRC), downstream of the TPC to be monitored. This monitoring solution was added retrospectively to the existing TPC system without a surgical operation to the chambers. A GRC was cost-effectively realized by using a MWPC designed to be compatible with existing TPC readout electronics. In such a way the development time and cost of the readout electronics could be spared. In order to match such an MWPC to the TPC readout electronics, it was necessary to slow down the signal formation in the GRC, since TPC readout electronics typically allows for a considerable trigger delay. This signal slowing was achieved by using an adjustable drift field transverse to the particle passage direction. The number of required readout channels was minimized using Cartesian readout. Since the NA61/SHINE experiment is used to study both low- and high-multiplicity collisions, the acceptance of the GRC was designed to be sufficiently large while addressing the issue of combinatorial ghost hits. The latter was handled by making the acceptance adjustable: when studying high-multiplicity collisions, individual sense wires can be switched off down to a single wire, eliminating the Cartesian ghosts, whereas for low-multiplicity runs the full acceptance is used with all of the sense wires operational.

The GRC system has been demonstrated of being capable of monitoring the drift velocity down to a one permil absolute precision in about 5 minute time windows. That is, the pertinent method is applicable to large drift length TPC systems, with minimal design time, and relatively low manpower and cost.

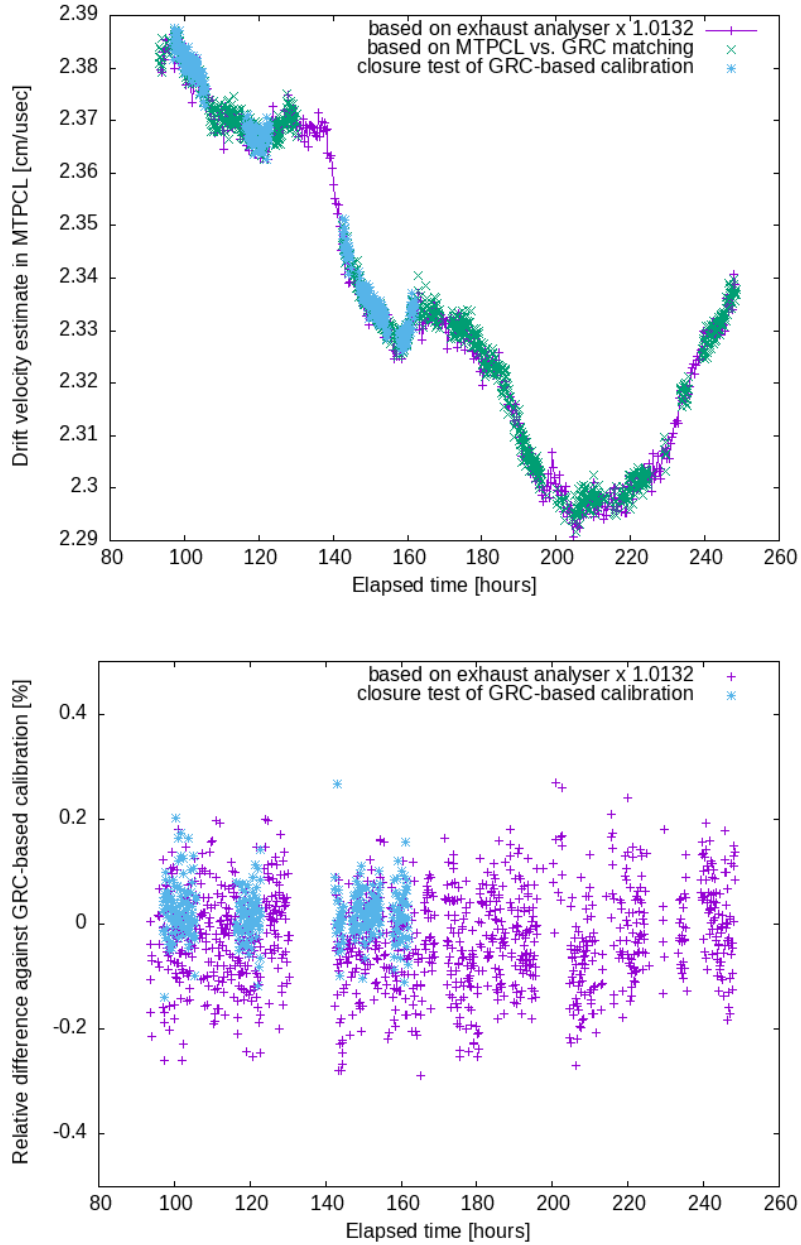


Figure 6. (Color online) Top panel: final validation of the GRC-based Δy versus y drift velocity calibration method. Statistical uncertainties of the data points are below 0.05%, therefore errorbars are not shown. It is seen that the closure test is satisfied to the desired accuracy (1-2 permil). That provides an empirical estimate for the systematic uncertainties. Moreover, consistency is seen with the exhaust analyzer method, up to a scale adjustment factor of 1.0132. Note that the exhaust analyzer method is expected to have some absolute systematic error, which explains the necessity for the empirical scale adjustment factor. Bottom panel: the same data points, shown in terms of relative difference with respect to the GRC-based calibration method.

Motivated by the GRC-based drift velocity monitoring method, a calibration procedure for the other geometric calibration parameters of the NA61/SHINE TPC chambers was also developed.

Using that concept, all 8 parameters (time-dependent drift velocity, trigger delay, alignment shifts, and alignment angles) of the TPC system were successfully calibrated, for each chamber.

Acknowledgements

We thank to the members of the REGARD gaseous R&D group at the Wigner RCP, moreover for the support and cooperation from the members of the NA61/SHINE Collaboration at CERN, in particular to Bartosz Maksiak, Wojciech Bryliński and Kyle Allison.

This work was supported by the Hungarian Scientific Research Fund (NKFIH OTKA-K138136-K138152, OTKA-FK135349 and TKP2021-NTKA-10). Detector construction and testing was completed within the Vesztergombi Laboratory for High Energy Physics (VLAB) at HUN-REN Wigner RCP.

Appendix

A Trigger delay and drift-direction alignment of TPCs

After the drift velocity has been calibrated with the Δy versus y method, one has $v_{\text{drift,nom}} \approx v_{\text{drift,true}}$, and therefore the TPC-GRC drift coordinate mismatch becomes y -independent, expressible as

$$\Delta y = \underbrace{(t_{0,\text{true}} - t_{0,\text{nom}})}_{\text{slope}} \cdot v_{\text{drift}} + \underbrace{(y_{\text{anode,nom}} - y_{\text{anode,true}})}_{\text{offset}} \quad (\text{A.1})$$

as seen from Eq.(4.2). Taking several data samples with actual drift velocity differing by 2–3%, the slope of the Δy versus v_{drift} scatter plot provides an estimate for the additive correction between the true trigger delay ($t_{0,\text{true}}$) and the trigger delay rough estimate applied during the initial reconstruction ($t_{0,\text{nom}}$). Thus, $t_{0,\text{true}}$ can be estimated from the TPC-GRC mismatch data. After the t_0 is calibrated, the TPC-GRC mismatch will be not only y -independent, but also v_{drift} -independent, and one is left with $\Delta y = y_{\text{anode,nom}} - y_{\text{anode,true}}$. Thus, the drift direction displacement (y -alignment correction) $y_0 := y_{\text{anode,nom}} - y_{\text{anode,true}}$ of the TPC versus the GRC can be estimated from the TPC-GRC mismatch data. An example for the Δy versus v_{drift} calibration method is shown in Fig.7. Having the t_0 and y_0 obtained, the upstream TPC chambers can also be calibrated, using the already calibrated TPCs as geometry reference, in place of the GRC.

In the calibration database, for each TPC, the t_0 information is stored as follows. The t_0 for one of the TPCs (MTPC-L) is stored as a global reference (called to be the global t_0). For the other TPCs, only their relative t_0 difference with respect to this reference TPC is stored (called to be the chamber t_0). The rationale in such separation of the global and chamber t_0 contributions is the following. The chamber t_0 values are supposed to be detector constants, as they can only depend on cable lengths and electronic delays with respect to the trigger system. The global t_0 , however, can also depend on the physics settings, such as beam time-of-flight, custom settings of delays inside the trigger logic etc. Thus, it is safer to recalibrate the global t_0 (MTPC-L versus GRC) for each data taking campaign, whereas it is enough to determine the relative chamber t_0 constants (other TPCs versus MTPC-L) only once, as they are detector constants. The recalculated relative chamber t_0 values are used, though, for consistency checks and quality monitoring.

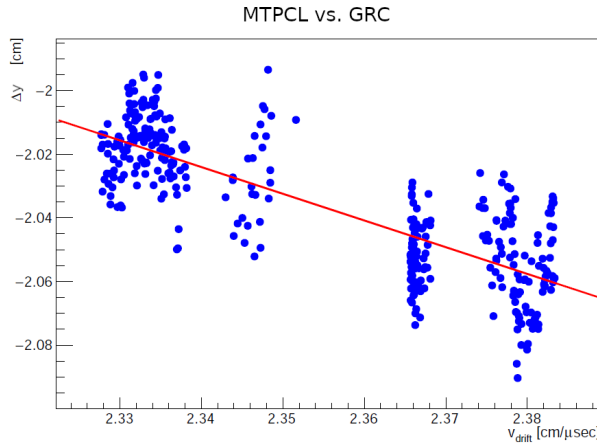


Figure 7. (Color online) An example for the Δy versus v_{drift} analysis for trigger delay (t_0) and drift direction shift (y_0) calibration, after the drift velocity (v_{drift}) has been obtained. The slope of the pertinent scatter data gives the t_0 correction, whereas the offset gives the y_0 correction. For the method to be workable, data samples with different drift velocities (up to 2 – 3%) are used. The pertinent data set is a high multiplicity collision type (Pb+Pb collisions at 150 AGeV/ c beam momentum, recorded in 2022).

B Systematic errors and alignment calibration of the TPCs

As summarized in Section 4, the final systematic errors of the in-situ drift velocity calibration via the Δy versus y method was verified to be not worse than 1-2 permil (or 1 mm overall, along the ~ 1 m drift length). This performance, however, was achievable after some detailed studies. Since the adjacent TPCs are calibrated against each-other (with first MTPC-L being calibrated against the GRC), the main source of systematic errors is the possible misalignment of the adjacent chambers (or the misalignment of MTPC-L versus the GRC). Considering a pair of adjacent chambers, one of which is an already fully calibrated chamber or the GRC, the other being an uncalibrated TPC, evaluation of affine transformations show that the track-by-track systematic error in the multiplicative drift velocity correction $v_{\text{drift,corr}} := v_{\text{drift,true}}/v_{\text{drift,nom}}$ caused by misalignment is

$$\text{syst}(v_{\text{drift,corr}}) = \left(y \cdot \theta_x + x \cdot \theta_y + (y - y_{\text{mainvertex}}) \cdot \theta_x + z_0 \right) \cdot \frac{1}{z - z_{\text{mainvertex}}}, \quad (\text{B.1})$$

to the first order.⁵ Here, x, y, z is the particle hit position at the $z = \text{const}$ reference plane of the Δy versus y study (e.g. the GRC plane), moreover x_0, y_0, z_0 denote the (unknown) correction to the position alignment of the uncalibrated chamber, and $\theta_x, \theta_y, \theta_z$ denote the (unknown) correction to the angular alignment of the uncalibrated chamber, whereas the x, y, z coordinates indexed by $(\)_{\text{mainvertex}}$ denote the coordinates of the collision point. It is seen that the alignment caused drift velocity systematic error decreases with distance from the main-vertex, and therefore justifies our

⁵This identity can be derived analytically, for magnetic field-off data, i.e. for straight tracks. Since the drift directions of the NA61/SHINE TPCs approximately coincide with the direction of the magnetic bending field, i.e. the drift and the bending does not interfere to the first order, the formula holds for magnetic field-on data as well, to a good approximation. In order to aid the tedious analytic evaluation of the three dimensional affine transformations, automatic formula manipulation software was used (the LinearAlgebra package of Maple).

placement of the GRC downstream of all the TPCs, as seen in Fig.2. Even if the alignment of the MTPC-L with respect to the GRC were imperfectly known to $|y \cdot \theta_x| \lesssim 1$ cm or $|x \cdot \theta_y| \lesssim 1$ cm or $|(y - y_{\text{mainvertex}}) \cdot \theta_x| \lesssim 1$ cm or $|z_0| \lesssim 1$ cm, this would not disturb the MTPC-L versus GRC drift velocity calibration beyond half permil, since $|z_{\text{GRC}} - z_{\text{mainvertex}}| \approx 16$ m is large. That is, the alignment imperfection does not give sizable systematic error to the MTPC-L versus GRC drift velocity calibration. When propagating the drift velocity calibration toward the upstream chambers (VTPC-1, VTPC-2), however, the systematic error Eq.(B.1) by imperfectly known alignment can give a sizable contribution. Therefore, in this appendix we briefly describe, how the alignment is calibrated.

A TPC chamber has in total 8 unknown calibration coefficients related to its geometry: the x_0, y_0, z_0 position misalignment correction (transverse, drift direction, longitudinal), the $\theta_x, \theta_y, \theta_z$ angular misalignment correction, the drift velocity correction ($v_{\text{drift,corr}} - 1$), and the correction to the trigger delay $t_{0,\text{corr}} := t_{0,\text{true}} - t_{0,\text{nom}}$. These unknown imperfection parameters, to be determined by the calibration procedure, are small, and therefore correction to the first order Taylor expansion terms with respect to these is enough. We use special magnetic field-off calibration runs in order to have only straight trajectories for charged particle tracks throughout the chamber system. In other words, a tomography of the chamber system is done using an ensemble of straight global tracks associated to the main-vertex, and their mismatch pattern is studied when dissected and refitted by straight lines in the local detectors, as illustrated in Fig.8.

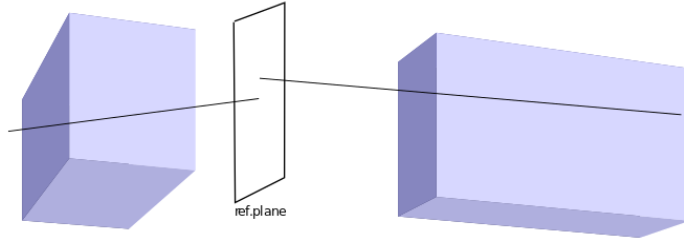


Figure 8. (Color online) Sketch of the alignment calibration strategy for adjacent TPCs: special magnetic field-off alignment calibration runs are recorded, i.e. a tomography of the chamber system is performed by straight global main-vertex tracks. If the relative alignment parameters for the chambers assumed during the reconstruction are imperfect, the track parameters will have a mismatch, when compared on a joint reference plane, for the adjacent chambers.

Quantitatively, the magnetic field-off data based alignment calibration goes as follows. For MTPC-L, the $(v_{\text{drift,corr}} - 1)$ parameter is determined as in Section 4, and the parameters $t_{0,\text{corr}}, y_0$ are determined as in Appendix A, whereas $\theta_x = \theta_y = \theta_z = 0$ and $x_0 = z_0 = 0$ by convention, i.e. MTPC-L is taken as alignment reference. The other chambers are calibrated against each-other pairwise, for all the 8 parameters, assuming that one in the pair is already calibrated. In order to fix sign conventions, in this section it is assumed that the downstream chamber is calibrated, but analogous calibration equations hold when the upstream chamber is the calibrated one. An imperfection in the assumption about the 8 parameters of the upstream chamber causes a mismatch between locally

refitted track pieces in the adjacent chambers, when compared on a $z = \text{const}$ reference plane, see again Fig.8. If the straight track segments are parameterized by the four parameters N_x, N_y, M_x, M_y as $x(z) = M_x + (z - z_{\text{ref}}) \cdot N_x$ and $y(z) = M_y + (z - z_{\text{ref}}) \cdot N_y$, then the locally refitted and compared local tracks will give a track parameter mismatch vector field $\Delta N_x, \Delta N_y, \Delta M_x, \Delta M_y$ as a function of the track parameters N_x, N_y, M_x, M_y in the downstream chamber (which is already calibrated or reference). Evaluating affine transformations, one arrives at the formula

$$\begin{aligned}
\Delta N_x &= (1 + N_x^2) \cdot \theta_y + N_y \cdot (N_x \cdot \theta_x + \theta_z), \\
\Delta N_y &= N_y^2 \cdot (\theta_x + \theta_y) + N_y \cdot (v_{\text{drift,corr}} - 1) - N_x \cdot \theta_z + \theta_x, \\
\Delta M_x &= N_x \cdot (M_y \cdot \theta_x + M_x \cdot \theta_y + z_0) + z_{\text{ref}} \cdot \theta_y + M_y \cdot \theta_z - x_0, \\
\Delta M_y &= N_y \cdot (M_x \cdot \theta_y + M_y \cdot \theta_x + z_0) + z_{\text{ref}} \cdot \theta_x - M_x \cdot \theta_z - y_0 \\
&\quad + (M_y - y_{\text{anode,nom}}) \cdot (v_{\text{drift,corr}} - 1) - t_{0,\text{corr}} \cdot v_{\text{drift,nom}}
\end{aligned} \tag{B.2}$$

for the mismatch field, to the first order, given the 8 imperfection parameters $\theta_x, \theta_y, \theta_z, x_0, z_0, (v_{\text{drift,corr}} - 1), t_{0,\text{corr}}, y_0$. For practical reasons, the track sample satisfying $|N_y| \approx 0$, i.e. close to horizontal tracks are used, since for these the first two lines of Eq.(B.2) simplifies as

$$\begin{aligned}
\text{for } |N_y| \approx 0, \text{ one has :} \\
\Delta N_x &= (1 + N_x^2) \cdot \theta_y, \\
\Delta N_y &= -N_x \cdot \theta_z + \theta_x.
\end{aligned} \tag{B.3}$$

That is, for magnetic field-off data, for $|N_y| \approx 0$ main-vertex tracks, from the ΔN_x versus N_x plot the parameter θ_y can be read off, whereas from the ΔN_y versus N_x plot the parameters θ_x and θ_z can be read off, see Fig.9 top panels. After re-reconstructing with the obtained $\theta_x, \theta_y, \theta_z$ angular alignment corrections, the third line of Eq.(B.2) yields

$$\Delta M_x = N_x \cdot z_0 - x_0. \tag{B.4}$$

That is, for magnetic field-off data, from the ΔM_x versus N_x plot the parameters x_0 and z_0 can be read off, see Fig.9 bottom panel.

After re-reconstruction with the obtained $\theta_x, \theta_y, \theta_z$ angular alignment corrections and the x_0, z_0 alignment shift corrections, the fourth line of Eq.(B.2) yields

$$\Delta M_y = M_y \cdot (v_{\text{drift,corr}} - 1) - y_{\text{anode,nom}} \cdot (v_{\text{drift,corr}} - 1) - t_{0,\text{corr}} \cdot v_{\text{drift,nom}} - y_0 \tag{B.5}$$

which is nothing but the already known Eq.(4.2), to the first order in $(v_{\text{drift,corr}} - 1)$, re-expressed in the notations of this appendix. That is, the drift velocity correction $(v_{\text{drift,corr}} - 1)$ can be determined via the usual Δy versus y method, as already described in Section 4. Finally, after re-reconstruction, one arrives at

$$\Delta M_y = -t_{0,\text{corr}} \cdot v_{\text{drift,nom}} - y_0, \tag{B.6}$$

which is nothing but the already known Eq.(A.1), re-expressed in the notations of this appendix. Therefore, the remaining corrections $t_{0,\text{corr}}$ and y_0 can be determined via the usual Δy versus v_{drift} method, as already described in Appendix A. Thus, the triangular system of calibration equations for the 8 TPC geometry unknowns is saturated, and the entire TPC system can be calibrated.

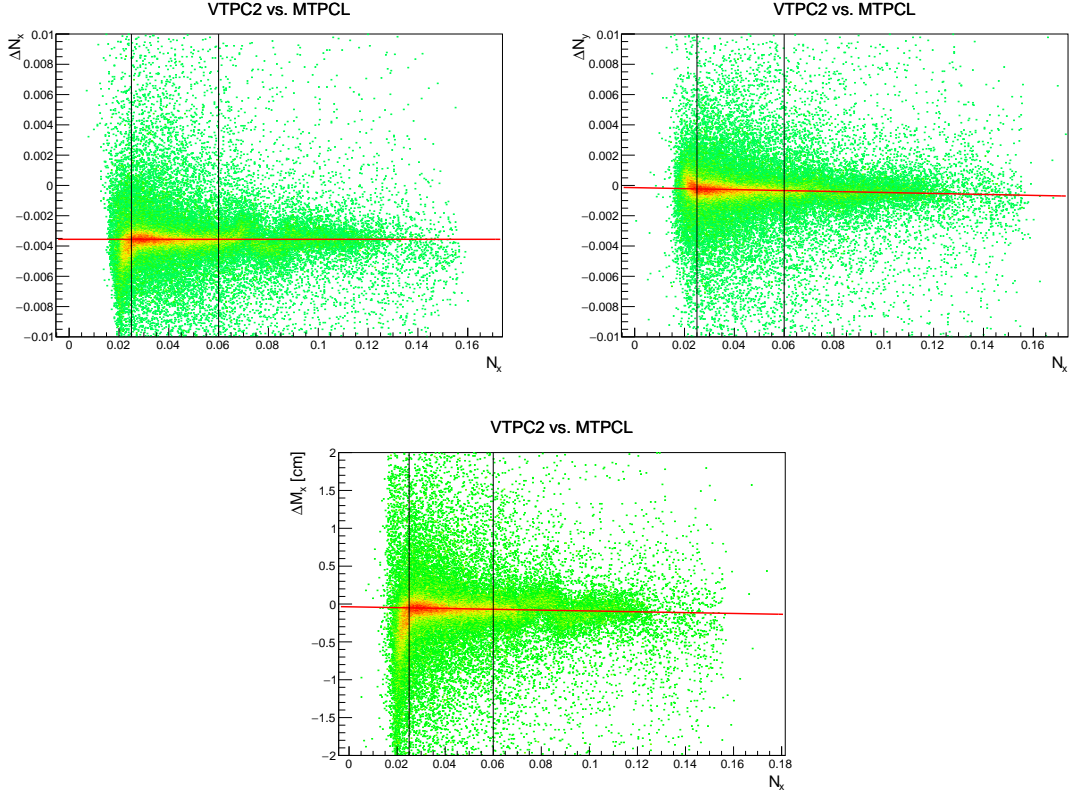


Figure 9. (Color online) Top panels: an example for the $\theta_x, \theta_y, \theta_z$ angular alignment calibration using ΔN_x versus N_x and ΔN_y versus N_x plots for $|N_y| \approx 0$ tracks in magnetic field-off data (the pertinent sample is Pb+Pb at 150 AGeV/ c beam momentum, recorded in 2022). Bottom panel: an example for the x_0, z_0 position alignment calibration using ΔM_x versus N_x plot for tracks in magnetic field-off data (using the same sample as for the top panels). The black vertical lines indicate fiducial cuts, in order to avoid regions close to the TPC field cages, where the drift electric field can be imperfect (inhomogeneous). The color scale of the scatter plots is merely for emphasizing hit density for the eye. The line on the plots corresponds to a straight line fit to the scatter data, using the background tolerant LTS method.

After the full alignment correction, drift velocity correction, t_0 correction, y_0 correction, the overall systematic uncertainty of the geometry related calibration parameters of the large TPCs, as estimated via closure tests, are listed in Table 2. The statistical uncertainties of the parameters are negligible.

	$\theta_x, \theta_y, \theta_z$ [°]	x_0, z_0 [mm]	v_{drift} [%]	t_0 [ns]	y_0 [mm]
	syst.	syst.	syst.	syst.	syst.
MTPC-L	0 (reference)	0 (reference)	0.2	11	0.15
VTPC-2	0.038	0.30	0.2	33	0.25
MTPC-R	0.014	0.20	0.2	33	0.63
VTPC-1	0.026	0.25	0.2	32	0.07

Table 2. The table of overall systematic uncertainties of the TPC geometry parameters, for the large chambers, as estimated via closure tests. The calibration scheme was GRC \rightarrow MTPC-L, followed by MTPC-L \rightarrow VTPC-2, then VTPC-2 \rightarrow MTPC-R and VTPC-2 \rightarrow VTPC-1.

References

- [1] N. Abgrall et al. (the NA61 Collaboration), *NA61/SHINE facility at the CERN SPS: beams and detector system*, JINST **9** (2014) P06005 [arXiv:1401.4699].
- [2] K. Abe et al. (the T2K Collaboration), *The T2K experiment*, Nucl. Instrum. Meth. **A659** (2011) 106 [arXiv:1106.1238].
- [3] B. Abi et al. (the DUNE Collaboration), *Deep Underground Neutrino Experiment (DUNE), Far Detector Technical Design Report, Volume I: Introduction to DUNE*, JINST **15** (2020) T08008 [arXiv:2002.02967].
- [4] D. S. Ayres et al. (the NOvA Collaboration), *The NOvA Technical Design Report*, FERMILAB-DESIGN-2007-01 [doi:10.2172/935497].
- [5] K. Abe et al. (the Hyper-Kamiokande Collaboration), *Hyper-Kamiokande Design Report*, [arXiv:1805.04163].
- [6] A. Aab et al. (the Pierre Auger Collaboration), *The Pierre Auger Cosmic Ray Observatory*, Nucl. Instrum. Meth. **A798** (2015) 172 [arXiv:1502.01323].
- [7] M. Kuich, *Kaon production in mid-rapidity in Be+Be collisions at the CERN SPS*, PhD thesis, University of Warsaw (2019), sections D.4 and D.5 [EDMS:2150851].
- [8] S. Afanasiev et al. (the NA49 Collaboration), *The NA49 large acceptance hadron detector*, Nucl. Instrum. Meth. **A430** (1999) 210.
- [9] A. Cattai, H. G. Fischer, A. Morelli, *Drift velocity in Ar + CH₄ + water vapours*, DELPHI Internal Report (1989) 63.
- [10] W. B. Atwood et al., *Performance of the ALEPH Time Projection Chamber*, Nucl. Instrum. Meth. **A306** (1991) 446.
- [11] C. Brand et al., *The DELPHI time projection chamber*, IEEE Transactions on Nucl. Science **36** (1989) 122.
- [12] J. Alme et al., *The ALICE TPC, a large 3-dimensional tracking device with fast readout for ultra-high multiplicity events*, Nucl. Instrum. Meth. **A622** (2010) 316 [arXiv:1001.1950].
- [13] J. Abele et al., *The Laser System for the STAR Time Projection Chamber*, Nucl. Instrum. Meth. **A499** (2003) 692.
- [14] M. Anderson et al., *The STAR Time Projection Chamber: a unique tool for studying high multiplicity events at RHIC*, Nucl. Instrum. Meth. **A499** (2003) 659.

- [15] D. Varga, G. Nyitrai, G. Hamar, L. Oláh, *High efficiency gaseous tracking detector for cosmic muon radiography*, *Advances in High Energy Physics* **2016** (2016) 1962317 [[arXiv:1607.08494](#)].
- [16] D. Varga, Sz. J. Balogh, Á. Gera, G. Hamar, G. Nyitrai, G. Surányi, *Construction and readout systems for gaseous muography detectors*, *J. Adv. Instrum. in Science* **2022** (2022) 307.
- [17] R. Sipos, A. László, A. Marcinek, T. Paul, M. Szuba, M. Unger, D. Veberic, O. Wyszynski, *The offline software framework of the NA61/SHINE experiment*, *J. Phys. Conf. Ser.* **396** (2012) 022045.
- [18] R. Brun, F. Rademakers, *ROOT – An object oriented data analysis framework*, *Nucl. Instrum. Meth.* **A389** (1997) 81.
- [19] “ROOT” software [[doi : 10.5281/zenodo.848818](#)].